SolarPACES 2023, 29th International Conference on Concentrating Solar Power, Thermal, and Chemical Energy Systems

Analysis and Simulation of CSP and Hybridized Systems

https://doi.org/10.52825/solarpaces.v2i.815

Published: 28 Aug. 2024

Advanced Feedforward Controller for a Molten Salt Receiver in Star Design Based on Real-Time Flux Measurement

Jonas Schulte[1], Christian Schwager[1], Cristiano J. Teixeira Boura[1], and Ulf Herrmann[1]

[1] Solar-Institut Jülich of the FH Aachen University of Applied Sciences, Germany

*Correspondence: Jonas Schulte, j.schulte@sij.fh-aachen.de

Abstract. This paper presents a control system with a panel-wise applied feedforward temperature controller for a molten salt receiver in star design utilizing temperature measurements in the connecting pipes between the panels and a real-time flux density measurement as inputs. It is tested in realistic cloud passage scenarios and the results are compared to the results from an earlier developed control system for the same receiver, in which the temperature controller is based on a simple feedback controller (PID) supported by a simple feedforward controller. The results show that the performance of the new feedforward controller is outstanding and could be applied to common cylindrical receiver designs as well. Nevertheless, the highly increased actuator movement of the control valves is to be further investigated.

Keywords: Molten Salt Receiver, Star Design, Feedforward Controller, Model Predictive Control, Cloud Passages

1. Introduction

Controlling the temperature of molten salt receivers during cloud passage scenarios remains a challenging topic regarding the process control of molten salt solar towers (MST). A well-performing control system not only ensures a higher safety during operation under fluctuating solar conditions but also increases the efficiency of the receiver, as it allows for a higher outlet temperature setpoint. One of the main reasons controlling the receiver's outlet temperature is so challenging is the long residence time of the molten salt in the receiver, which varies between one and ten minutes depending on the mass flow rate [1, 2]. This is why conventional feedback controllers struggle, especially at low part loads. Although model-predictive controllers (MPC) are a promising solution for this issue, MPCs are complex and highly rely on accurate modeling and significant computing resources. In contrast, this work presents a panel-wise applied feedforward controller for a molten salt receiver in star design [3], which tackles the issue of the long residence times by using temperature measurements in the connecting pipes between panels as one of the inputs, as well as real-time flux measurement. This approach potentially leads to a better performance than conventional feedback controllers with much less complexity compared to an MPC. The star receiver is a receiver with three wings/cantilevers, which enable the irradiation of absorber tubes from both sides. This idea originates at the Institute for Solar Research at the DLR [3, 4]. A schematic of the star design is shown in Figure 1. For this work, it is assumed that the star receiver is equipped with a real-time flux density measurement system with a sufficiently high resolution that enables deriving panel-wise (intercept) flux. Corresponding flux density measurement systems [5–8] or heliostat

field calibration systems that can also be used for this purpose like “Method A” by Sattler et al. [9] are already known from research or are currently under development.

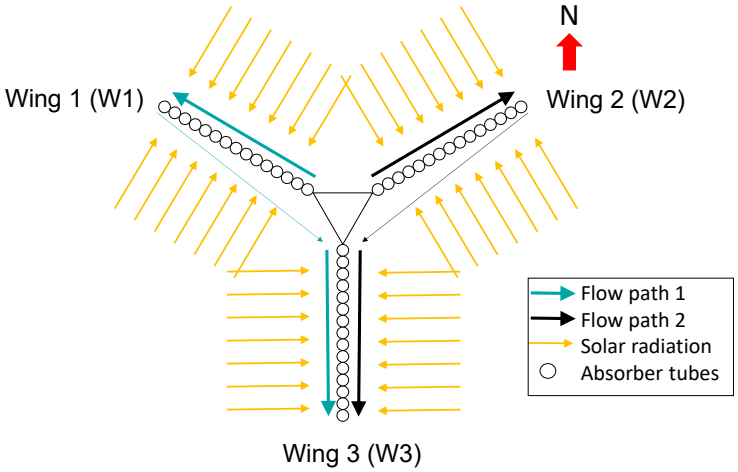

Figure 1. *Schematic sketch of a receiver in star design*

2. Approach and governing equations

The feedforward controller is developed for a receiver in star design as described in [3]. The design of the control concept is taken from [10] and adapted by substituting the temperature feedback controller with the new feedforward controller. As a test environment, the detailed dynamic model from [10] is used which is based on previous research by Schwager et al. [11]. Figure 2 shows a simplified PFD of the investigated system.

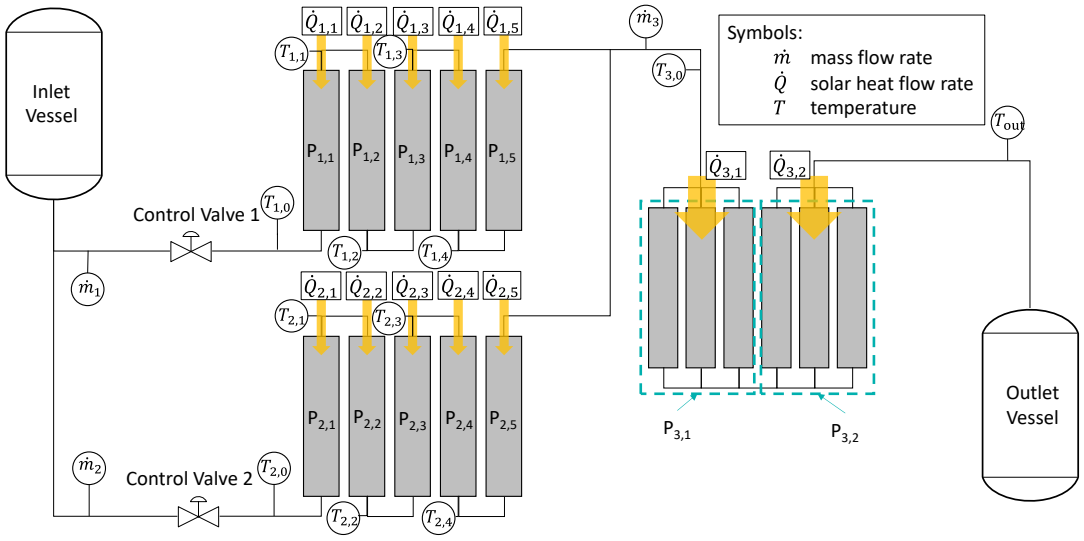

Figure 2. *Simplified PFD of the receiver system*

The approach of the feedforward controller is based on steady-state energy balances that are calculated from each panel outlet to the outlet of the receiver. That leads to several candidate values for the current mass flow rate, depending on the current flux distribution on the receiver. From these candidate values, the maximum is always taken as the receiver mass flow rate to ensure that the temperature setpoint is not exceeded. Applied to the system shown in Figure 2 this leads to the following equations, defining the mass flow signal of the feedforward controller:

$$\dot{m}_{\mathrm{ff}} = \max(\dot{m}_{\mathrm{cand},1,1}, \dots, \dot{m}_{\mathrm{cand},1,5}, \dot{m}_{\mathrm{cand},2,1}, \dots, \dot{m}_{\mathrm{cand},2,5}, \dot{m}_{\mathrm{cand},3,1}, \dot{m}_{\mathrm{cand},3,2}) \tag{1}$$

With the $\dot{m}_{\mathrm{cand},1}$ and the $\dot{m}_{\mathrm{cand},3}$ values defined as follows:

$$\dot{m}_{\mathrm{cand},1,i} = \frac{\eta_{\mathrm{th}}\left(\sum_{j=i}^{5}\frac{\dot{Q}_{1,j}}{x} + \dot{Q}_{3,1} + \dot{Q}_{3,2}\right)}{c_{\mathrm{p}}(T_{\mathrm{out,set}} - T_{1,i-1})} \quad i \in \mathbb{N} \mid 1 \leq i \leq 5 \tag{2}$$

$$\dot{m}_{\mathrm{cand},3,1} = \frac{\eta_{\mathrm{th}}(\dot{Q}_{3,1} + \dot{Q}_{3,2})}{c_{\mathrm{p}}(T_{\mathrm{out,set}} - T_{3,0})}; \quad \dot{m}_{\mathrm{cand},3,2} = \frac{\eta_{\mathrm{th}}\dot{Q}_{3,2}}{c_{\mathrm{p}}(T_{\mathrm{out,set}} - T_{3,1})} \tag{3}$$

The definition of the $\dot{m}_{\mathrm{cand},2}$ values is analogous except that x is replaced by $(x-1)$. In this equation, η_{th} is a function for the thermal efficiency characteristics of the receiver and x is the approximated mass flow distribution ratio between the first two wings of the receiver, which is defined as:

$$x = \frac{\dot{m}_1}{\dot{m}_1 + \dot{m}_2} \approx \frac{\sum_{i=1}^{5}\dot{Q}_{1,i}}{\sum_{i=1}^{5}\dot{Q}_{1,i} + \sum_{i=1}^{5}\dot{Q}_{2,i}} \tag{4}$$

The first simulations with a generic test scenario consisting of various flux steps on the receiver and the new feedforward controller, without any feedback, showed that there is always a steady state control error depending on the state of load of the receiver. Figure 3 shows the test scenario and the resulting outlet temperature of the receiver.

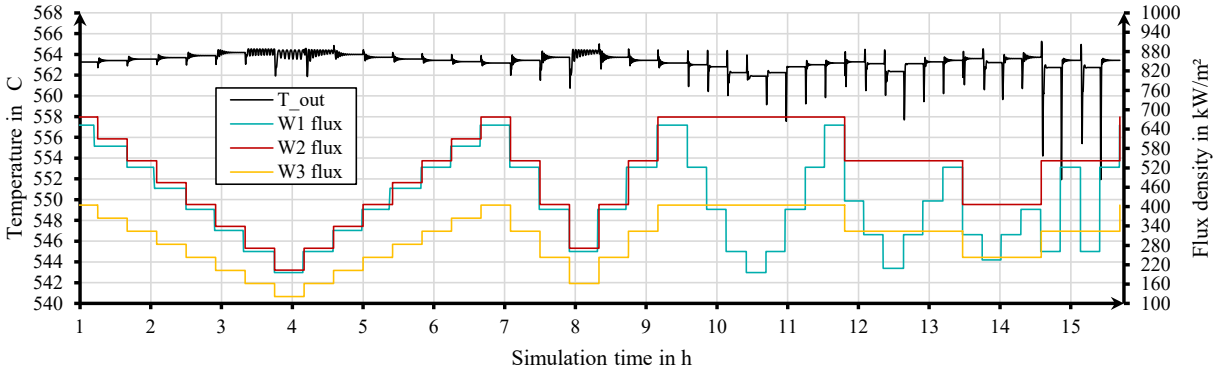

***Figure 3**. Generic test scenario of flux steps on the receiver and the resulting outlet temperature trends for a plain feedforward temperature controller*

It can be seen, that the outlet temperature is always lower than the outlet temperature setpoint of 565 °C. This is due to inaccuracies in the used function for the receiver's thermal efficiency characteristics. As mentioned before, the steady state control error depends on the load conditions of the receiver. It varies depending on the overall flux on the receiver and also on the flux distribution. These interdependencies are too complex to be addressed by simple analytic approaches. Hence, a feedback loop is needed. Although the most intuitive approach is to correct the mass flow signal of the feedforward controller with a feedback controller, this was not an option because, in combination with this feedforward controller, it leads to extensive system instability. So, the temperature setpoint was chosen as the preferred value to be adapted by a feedback controller with an integrating component. This leads to the control system shown in Figure 4. The controller chosen for this purpose is a simple I controller, which corrects the setpoint slightly. The resulting manipulated setpoint is then fed to the feedforward controller.

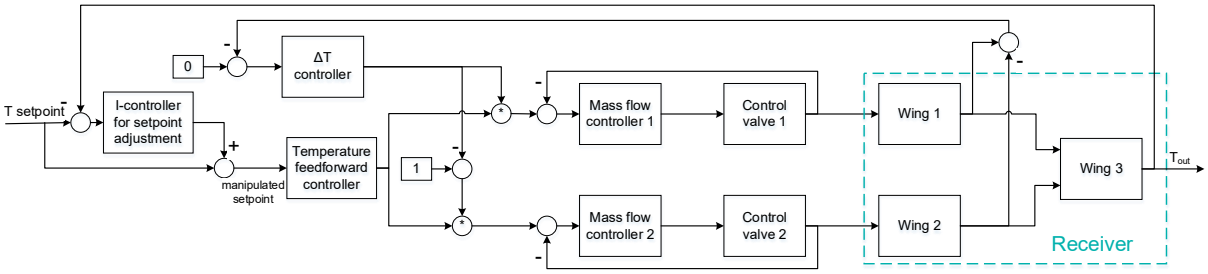

***Figure 4**. Control system of the receiver with panel-wise feedforward*

Figure 3 also shows that the system with the feedforward controller tends to exhibit low-frequency oscillations with small amplitude. These oscillations seem to be no problem for the system stability. Nevertheless, they lead to unnecessary actuator movement of the control valves, which is undesirable.

3. Cloud passage test scenario

For testing the feedforward controller under realistic radiation conditions the test scenario from [10] was adopted. It is based on DNI-maps of an 8x8 km² area with a spatial resolution of 20x20 m² and a time resolution of 30 s. The DNI-maps are sourced from an all-sky-imager based nowcasting system by Nouri et al. [12]. To convert these DNI-maps into a flux density distribution the heliostat field (30972 heliostats) is clustered into six parts. These parts are then assigned to different areas on the receiver (the optical height of the receiver is 200 m). Accordingly, the nominal flux density distribution is scaled depending on the area-weighted average of the Clear Sky Index (CSI) in the area of each heliostat field cluster. This method leads to the flux trends shown in Figure 5.

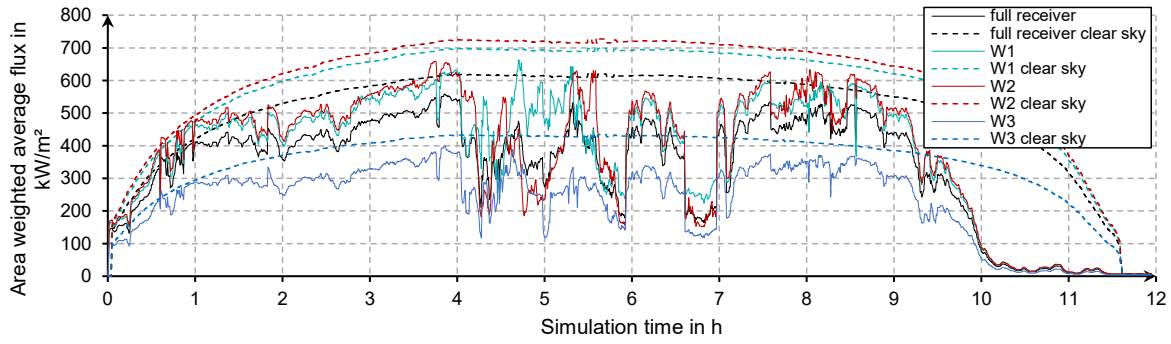

***Figure 5**. Resulting flux trends of the cloud passage test scenario*

4. Test results

Since the results are most interesting when the control system is most challenged, Figure 6 only shows the time with the highest flux density fluctuations, which is in the time range of 3 - 7 h. To better assess the performance of the new control system, the results are compared with those from the optimized feedback controller with a simple feedforward controller that was developed in [10]. Figure 6 shows that the panel-wise feedforward controller achieves better results regarding temperature setpoint exceedances than the optimized feedback controller. Regarding setpoint undershoots, there is no significant difference noticeable.

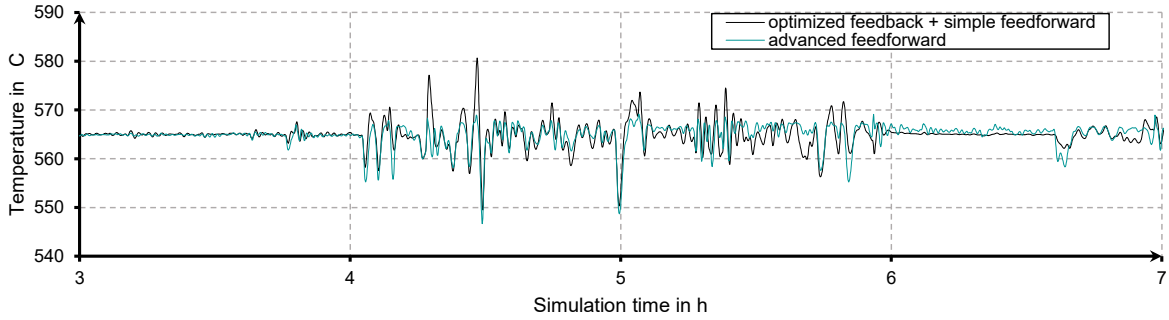

***Figure 6**. Outlet temperature trends of the receiver*

A statistical analysis of the control error is carried out to make this subjective impression objectively measurable. Since slight deviations between the setpoint and the measured value during changing conditions are inevitable and until a certain threshold not critical, small control errors with an absolute value of less than 4 K are neglected. The rest of the control errors is sorted into 2 K wide classes. The time in which these errors occur is integrated over the whole day. Figure 7 shows the results of this analysis. Setpoint undershoots are considered negative control errors and overshoots are vice versa. The results are compared to the results from the control system presented in [10] (optimized feedback + simple feedforward).

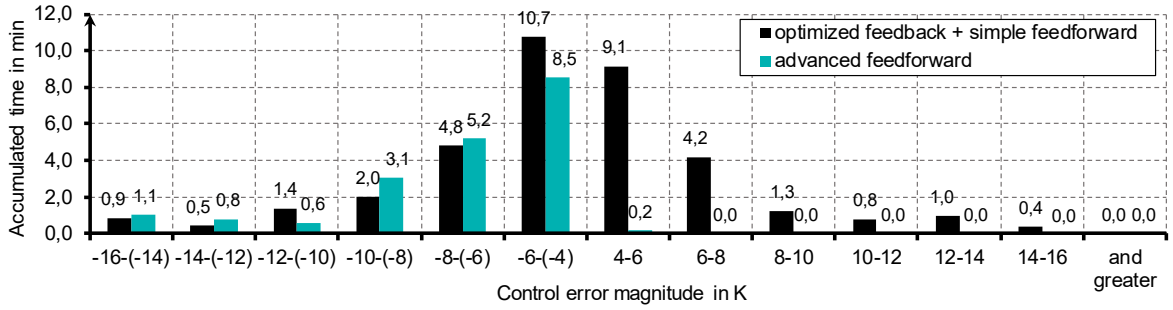

***Figure 7**. Accumulated time in which different control errors occur*

The statistical analysis supports the impression that the new feedforward controller can avoid temperature setpoint exceedances effectively. Regarding undershoots there is no significant difference between the two approaches. Overall the controller shows an excellent performance, almost totally avoiding critical setpoint exceedances.

One of the potential weaknesses of the new feedforward controller is that it tends to cause uncritical low-frequency oscillations, which cause unnecessary and undesirable actuator movements of the control valve. To gain an impression of how big the difference of the amount of actuator movements is compared to a system with a conventional feedback controller (PID) all actuator movements of the control valves are integrated for both the new control system and the system from [10]. The comparison reveals that the control valves make about 50 % more movement (time integral of all actuator movements) when the new feedforward controller is used.

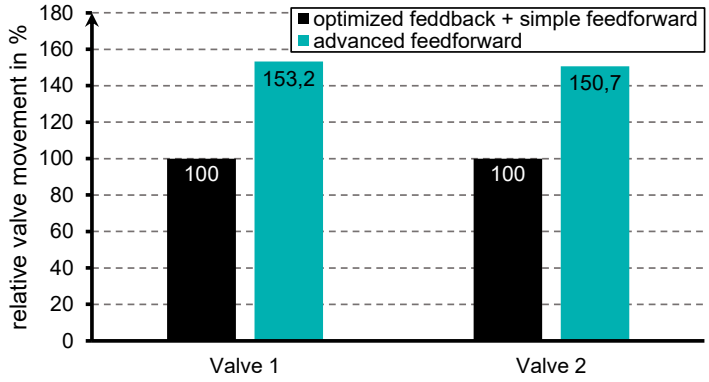

***Figure 8**. Accumulated relative valve actuator movement*

5. Conclusion

This paper presents a panel-wise applied feedforward controller that uses temperature measurements and panel-wise real-time flux measurement as inputs. The presented approach is much less complex than an MPC. Compared with control concepts that heavily rely on feedback controllers, the performance is outstanding. In a test over a whole day of operation with a realistic cloud passage scenario, the simulated temperature exceeded the setpoint by more than 4 K just for approximately 12 s. Even in moments with high flux gradients and high differences in the irradiation of the first to wings/cantilevers of the receiver, there are no setpoint violations that seem to be critical for safe operation of the plant. Since in contrast to the presented concept commercially applied control concepts often need to work with higher mass flow than needed during cloud passages to avoid the risk of critical temperature exceedances, this control concept potentially leads to higher average receiver outlet temperatures and thus to higher plant efficiency.

Despite the excellent performance, the new control concept also has weaknesses. Especially during operational conditions with low loads, the control system tends to low-frequency and low-amplitude oscillations, which lead to increased actuator movement of the control valves. Although these oscillations do not seem to be a problem for system stability, they are still undesirable because they potentially shorten the lifetime of the control valve actuators. That is why further investigations need to be carried out on how much of the increased actuator movement shown in Figure 8 is evitable by appropriate damping measures without impairing the system performance too much.

Data availability statement

The applied data are subject to third-party IP and therefore not publically available.

Author contributions

J. Schulte: Conceptualization, Data curation, Formal Analysis, Funding acquisition, Investigation, Methodology, Software, Visualization, Writing – original draft; **C. Schwager:** Data curation, Funding acquisition, Methodology, Project administration, Supervision, Writing – review & editing; **C. J. T. Boura:** Project administration, Supervision, Writing – review & editing; **U. Herrmann:** Supervision, Writing – review & editing

Competing interests

The authors declare no competing interests.

Funding

This work is funded by the German Federal Ministry for Economic Affairs and Climate Action.

References

1. Flesch R, Maldonado D, Schwarzbözl P. Dynamic Modelling of Molten Salt Central Receiver Systems:41–2. doi:10.11128/arep.55.a55231.
2. Schwager C, Angele F, Schwarzbözl P, Boura CJT, Herrmann U. Model predictive assistance for operational decision making in molten salt receiver systems. SolarPACES Conference 2021. 2021:30020. doi:10.1063/5.0151514.
3. Frantz C, Schloms F, Kuhl M, Binder M, Schuhbauer C. Design and Cost Analysis of a Combined STAR and C-PV Molten Salt Receiver Concept for CSP Applications. SolarPACES Conference 2022. 2022.
4. Puppe M, Giuliano S, Frantz C, Uhlig R, Flesch R, Schumacher R, et al. Techno-economic optimization of molten salt solar tower plants. AIP Conference Proceedings 2018. doi:10.1063/1.5067069.
5. Raeder C, Offergeld M, Röger M, Lademann A, Zöller J, Glinka M, et al. Proof of concept: Real-time flux density monitoring system on external tube receivers for optimized solar field operation. SolarPACES Conference 2021:80008. doi:10.1063/5.0148725.
6. Göhring F, Bender O, Röger M, Nettlau, Janina, Schwarzbözl, Peter. Flux Density Measurment on Open Volumetric Receivers. Proc. of SolarPACES 2011;2011.
7. Röger M, Herrmann P, Ulmer S, Ebert M, Prahl C, Göhring F. Techniques to Measure Solar Flux Density Distribution on Large-Scale Receivers. Journal of Solar Energy Engineering 2014. doi:10.1115/1.4027261.
8. Offergeld M, Röger M, Stadler H, Gorzalka P, Hoffschmidt B. Flux density measurement for industrial-scale solar power towers using the reflection off the absorber:110002. doi:10.1063/1.5117617.
9. Sattler JC, Schneider IP, Angele F, Atti V, Teixeira Boura C, Herrmann U. Development of Heliostat Field Calibration Methods: Theory and Experimental Test Results. SolarPACES Conf Proc 2023. doi:10.52825/solarpaces.v1i.678.
10. Schulte J, Schwager C, Frantz C, Schloms F, Teixeira Boura CJ, Herrmann U. Control Concept for a Molten Salt Receiver in Star Design: Development, Optimization and Testing with Cloud Passage Scenarios. SolarPACES Conf Proc 2023. doi:10.52825/solarpaces.v1i.693.
11. Schwager C, Flesch R, Schwarzbözl P, Herrmann U, Boura CJT. Advanced two phase flow model for transient molten salt receiver system simulation. Solar Energy. 2022;232:362–75. doi:10.1016/j.solener.2021.12.065.
12. Nouri B, Blum N, Wilbert S, Zarzalejo LF. A Hybrid Solar Irradiance Nowcasting Approach: Combining All Sky Imager Systems and Persistence Irradiance Models for Increased Accuracy. Solar RRL. 2022;6:2100442. doi:10.1002/solr.202100442.